单缸低参数汽轮机末级排汽湿度的热力分析

田瑞峰

(哈尔滨工程大学 核科学与技术学院,黑龙江 哈尔滨 150001)

: 采用 VB 语言,通过动态链接库的调用,编制了低参数单缸汽轮机热力计算程序。 应用此程序,在不同设计参数下,针对无抽汽除湿、级间抽汽除湿和除湿级除湿3种方案,研究了机组末级湿度的变化。 结果表明,进汽压力、进汽温度和排汽压力三者对末级湿度的影响不同,进汽温度对末级湿度的影响最大,进汽压力次之,排气压力最小。在本研究所提参数条件下,满负荷运行很难保证末级出口湿度要求,需采用有效的内部除湿措施。 研究也表明,在不同位置抽汽除湿和除湿级除湿对机组末级湿度影响较大,在相同的设计参数下,在机组的第四级后抽汽除湿对机组末级湿度的影响最大。在相同的除湿效率下,除湿级位置每向后移动一级,使末级湿度降低约1%,随除湿级位置后移,除湿效率对末级湿度的影响增大。

:   ;   ;   ;

: TK262   : A

12%[1]。

[2]

[3]

1

VB ,   Windows

1.1

IAPWS-IF97 [4],

1.2

1.2.1 非调节级叶高的确定

[5],

1.2.2 非调节级焓降分配

[5],   :

$$\Delta h_{ai} = (D_i / D_1)^2 \Delta h_{an1} \tag{1}$$

: Δh_{an1} —   , kJ/kg; D_i — i , m; D_1 —   , m。

:

$$\Omega_i = 1 - (1 - \Omega_1) \cdot D_1 / D_i \tag{2}$$

: Ω_i — i ; Ω_1 —

1.2.3 非调节级进出口角度的确定

:

$$\alpha_{1(z-1)} = {}^{z-1}\!\sqrt{\alpha_z / \alpha_1}, \quad \beta_{2(z-1)} = {}^{z-1}\!\sqrt{\beta_z / \beta_1} \tag{3}$$

: $\alpha_{1(z-1)}$、$\beta_{2(z-1)}$ —   、   ; α_z、β_z —   ; α_1、β_1 —   。

1.2.4 级间抽汽除湿的处理

，

[6] 。   ，   。   [7]

5%   。   ，   1   。   ，

，   λ   [7]   。

:

$X_0(i)=X_b(i-1)+0.05×G_c/(G_0-G_c)$ (4)

$:X_0(i)-$; $X_b(i-1)-$

; G_0-

, kg/s; G_c- , kg/s。

， G_0-G_c。

图 1   湿蒸气区流量系数

1.2.5   除湿级的处理

，   。

，   ，

。   。

1.3

，

，   Φ   ，

Φ   :

$Φ=(y_1-y_2)/y_1$ (5)

$:y_1-$; y_2-

。

(5)   ，

，

1.2.6   流量系数的计算

，   ，

，   ，

。

[5] 。

，   ，

[7] :

$μ≈1+ΔT/T$ (6)

$: ΔT-$, K; $T-$

, K。

，   ，

，

图 2   低参数单缸汽轮机热力计算程序流程

，

2 。

2

2.1

3 ，

50 000 kW， 0.02 MPa，

280 ℃ 3.0 MPa ，

。 4

3.0 MPa， 280 ℃ ，

。 3 4

，

，

，

3 4 ， 、

，

，

0.1 MPa， 1

℃， 0.01 MPa ，

30%，

10%。

， 2.5～3.2 MPa， 0.016

～0.022 MPa， 250～305 ℃ ，

12%， 305 ℃ ，

， 12%。

，

12% ，

。

图 3 末级湿度随进口压力、温度变化

， 4

，
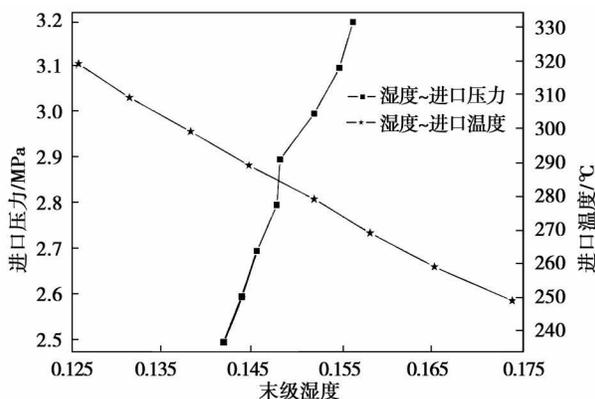
10 000 kW， 0.1%。

图 4 末级湿度随排汽压力、机组功率变化

2.2

5 50 000 kW， 3.0

MPa， 280 ℃、 0.02 MPa，

。 5 ，

， ，

， 8 ， 。

， ，

1% 。

0.01%，

。

， ，

， ，

。 [3] 1%～2%

，

[3]

， 。

5 ，

，

，

， ，

0.1% 。 3、 4 ，

， 2%

0.5%， 5% ，

12% ，

，

。

图 5 末级排汽湿度随抽汽量、抽汽位置变化

2.3

6   50 000 kW,   3. 0
MPa,   280 ℃、   0. 02 MPa,

7   ,

                     8 ,   ,

            ,   ,

1‰,

图 6 除湿级位置及除湿效率对末级排汽的影响

            7   ,
         ,   ,   0. 3 m,
      ,   ,   ,

            6   ,

                              10‰,
0.5‰ ~ 1‰,   ,
                          6   ,
                                           ,
         40‰   11. 5‰
         ,   12‰   。

图 7 各级动叶高度变化

3

                                       ,
         ,   、
   3   ,   。
              :
(1)   ,   、
                  ,

                  。

                  。
(2)
   ,   ,
               ,   5‰   ,
                  12‰   。
         [3]   1‰ ~ 2‰
                  。
(3)   ,
                  1‰。
         6   ,   ,

, 40％
12％ 。

:

[1] MOORE M J, SIVERDING C H. Two-phase steam flow in tubine and separators[R] . Washington; Hemisphere Publishing Corporation, 1976.

[2] , . [J] . , 1997, 17(2): 118－123.

[3] ДЕЙЧ М Е. Газодинамика решеток турбомашин[M] . Москва: Москва Энергоиздат, 1996.

[4] WAGNER W, COOPER J R, DITTMANN A. The IAPWS industrial formulation 1997 for the thermodynamic properties of water and steam[J] . Journal of Engineering for Gas Turbines and Power, 2000, 122(1): 150－182

[5] , . [M] . : , 1962.

[6] , , , . [J] . , 2005, 20(1): 1－5

[7] ТРОЯНОВСКИЙ Б М. Турбины Для атомных электростанций [M] . Москва: Энергоатомиздат, 1985.

（编辑 孙显辉）

据《Gas Turbine World》2009 年 3～4 月号报道, Saudi Electricity（沙特电力公司）投资 30 亿美元, 将在利雅得市郊建造一座现场额定输出功率为 2 000 MW PP10 电站（利雅得 10 号电站）。

该项目最初将安装并运行 36×Fr7EA 简单循环基本负荷燃气轮机, 以已处理过的原油作为燃料, 今后将转换成联合循环装置, 外加上不补燃的 HRSG（余热锅炉）和汽轮机发电机组。

——36×GE Energy PG 7121EA 快装式燃气轮机, 以天然气作为燃料, 每台燃气轮机的额定输出功率为 85.1 MW, 热效率为 32.70％, 36 台燃气轮机（电站）总的输出功率为 3 064 MW。

——在 50 ℃设计的环境温度下用已处理过的原油作为燃料, 每台燃气轮机的额定输出功率为 55.9 MW, 热效率为 29.90％, 电站总的输出功率为 2 012 MW。

——借助于加上 36×HRSG 和 9×110 MW 汽轮机, 把简单循环装置转换成联合循环装置, 以便使现场的额定输出功率增加到 3 000 MW。

——如同 PP9 装置（利雅得 9 号电站）, 利雅得 PP10 燃气轮机也将具有用不锈钢做成的烟囱、隔热管道和管道包壳, 以便防灰尘和耐腐蚀; 也装有针对十分高的沙尘而设计的自清洗入口过滤器。在转换成联合循环运行之前, 或在转换成联合循环运行时, 要给燃气轮机装上入口空气冷却装置, 以便针对夏季的峰荷运行增加电力生产。

目前, 利雅得地区 9 个电站总的装机功率约为 10 000 MW。在此项目完成后, 新的 PP10 项目（利雅得 10 号电站）将使该地区电站总装机功率增加约 20％, 以便满足规划的电力需求。沙特阿拉伯电力需求每年约增加 8％。

（ ）

the cold and hot fluid as well as solid walls. Studied was the response time of PSR during the period of the fluid flow rate undergoing a step change. Under the condition that the inlet parameters and heat quantity exchanged between the cold and hot air are identical and the flow rates at the cold and hot side have increased to three times of the original ones respectively, the response time of the PSR is only 1/8 of a shell-and-tube heat exchanger and 1/3 of a plate-fin type one. The numerical analytic results fully correspond to the test ones. As the time constant of the solid walls in the PSR is far less than that in a plate-fin type or a shell-and-tube recuperator, the response characteristics of the advanced recuperator with such a light weight structure are conspicuously superior to those of a conventional recuperator. **Key words:** gas turbine, primary surface recuperator, dynamic characteristics, numerical simulation

=**Analysis of the Mechanism Governing the Migration of Boundary Layers in a Highly-loaded Turbine Cascade Controlled By Using Bowed Blades**[,]/TAN Chun-qing, ZHANG Hua-liang (Engineering Thermophysics Research Institute, Chinese Academy of Sciences, Beijing, China, Post Code: 100190), HAN Wan-jin, WANG Zhong-qi (College of Energy Science and Power Engineering, Harbin Institute of Technology, Harbin, China, Post Code: 150001)//Journal of Engineering for Thermal Energy & Power. — 2009, 24(6). —700~704

Numerically simulated was the inner flow field in a highly-loaded plane turbine cascade with a turning angle of 128.5 degrees. In combination with the previous test results and by utilizing topological theory, the influence of bowed blades on the evolution of boundary layers and movement of vortices in the above-mentioned cascade was analyzed in detail. It has been found that the concentrated vortex system predominated by the passage vortices was drastically mixed and diluted in the middle portion of the highly-loaded turbine cascade and its energy loss coefficient (0.56) is conspicuously higher than that at both ends (0.07). This constitutes the underlying cause that negatively-bowed blades can improve the overall aerodynamic performance of a cascade. After a further discussion of boundary layer migration theory, it is noted that when the bowed blades are used in highly-loaded turbine cascades to reduce the secondary flow losses, the migration of free vortex layers should be investigated with focused attention. **Key words:** bowed blade, high load, flow separation, boundary layer migration, secondary flow, topology

= **Thermodynamic Analysis of the Last-stage Exhaust Steam Wetness of a Single-cylinder Low-parameter Steam Turbine**[,]/TIAN Rui-feng (College of Nuclear Science and Technology, Harbin Engineering University, Harbin, China, Post Code: 150001)//Journal of Engineering for Thermal Energy &Power. —2009, 24(6). —705~709

By adopting VB language and using a dynamic-link data base, designed was a thermodynamic calculation program for low-parameter single-cylinder steam turbines. By employing this program, the change of the last-stage wetness of the turbine unit for the following three versions of wetness removal was studied at various design parameters: namely, (1) without any steam extraction, (2) by extracting steam between stages and (3) by adopting a wetness removal stage. It has been found that the inlet steam pressure and temperature as well as the exhaust steam pressure can affect the last-stage wetness in different ways, and the inlet steam temperature exercises a maximal influence on the last-stage outlet wetness with consecutively less influence being exerted by the inlet steam pressure and the exhaust steam pressure. Under the given parameter condition of the present study, it is difficult for a full-load operation to meet the requirement for the last-stage outlet wetness, making it necessary to take effective inner wetness removal measures. The research results also indicate that the wetness removal by extracting steam at different locations, and by using a wetness removal stage exercises a relatively big influence over the last-stage wetness of the unit. At the same design parameters, the wetness removal by extracting steam after the fourth stage of the unit can maximally affect the last-stage wetness of the unit. At an identical wetness removal efficiency, when the location of the wetness removal stage shifts one stage backwards each time, it will lower the last-stage wetness by about 1%. With the location of the wetness removal stage moving backward, the influence of the wetness removal efficiency on the last-stage wetness will increase. **Key words:** single-cylinder steam turbine, thermodynamic design,

wetness removal stage, wetness removal efficiency

In the light of the features of rotors running at a high speed, analyzed was the air moving status in the air duct of the rotors with a numerical calculation model being established. The analytic results show that the air motion in the rotor air duct is the result of a joint action of the fan and rotor high speed rotation. With the ventilation structure of a suction type air-cooled turbogenerator serving as an example, a rotor rotating at a speed of 3 000 r/min can increase the air admission quantity of the air duct from 0. 14 kg/s to 0. 21 kg/s, and the influence of the rotor rotation on the air motion in the air duct must be taken into account. The inviscid version should be chosen for a viscid model. A comparison of model test results of the rotor air duct outlet air speed with the numerical simulation ones under same conditions indicates that the numerical simulation ones are in agreement with relevant engineering practice. A rational calculation model for the air motion flow field in the air duct of the rotors shall be as follows: the suction type fan and the inlet of the air duct of the rotor are used as the inlet and outlet boundary conditions, the rotor rotation is considered in the fluid boundary condition, the relative coarseness coefficient and constants in the wall boundary conditions which reflect the surface coarseness of the tube walls shall be $K_s^+ = 500 \sim 1000$ and $C_k = 1. 0$ respectively. An inviscid model would be chosen for the viscous model. The calculation model in question can be used to analyze the air motion flow field in the rotor air duct of the air-cooled turbogenerator. **Key words**: rotor turning, viscous model, air motion flow field in the air duct of a rotor

A comparison of the numerical calculation results of a transonic stationary cascade with the test ones shows that they are in relatively good agreement. To determine an appropriate aspect ratio for bowed and swept blades in a transonic compressor, numerically analyzed were the flow fields of the bowed and swept blades with 0 ~30 degrees having an aspect ratio of 1. 25, 1. 50 and 2. 00 respectively at an attack angle of 0 degree. It has been found that when the bowed and swept angle is set at 10 degrees, the bowed and swept blades with a small aspect ratio have a comparatively conspicuous influence on the blade performance. When the above-mentioned angle is 20 degrees, the blades with a big aspect ratio exercise a relatively obvious influence on the blade performance. The bowed and swept blades can make the shock waves at the leading edge being converted to oblique shock waves and weaken the intensity of the passage shock waves, thus reducing the shock wave losses of the cascade. It can be proven that the magnitude of the aspect ratio under the transonic conditions represents an important reference factor on how to use the bowed and swept blades. **Key words**: diffusion cascade, bowed and swept blade, turning angle, transonic compressor

On the basis of a design idea involving layered aerodynamic optimization of compressors, in combination with an optimization algorithm and CFD (computational fluid dynamics) techniques as well as a compressor aerodynamic design program,